Super-resolution atomic microscopy using orbit angular momentum laser with temporal modulation

Yuan Liu[1] and Dongxiao Li[1]

[1]*School of Physics, Institute for Quantum Science and Engineering, Huazhong University of Science and Technology, Wuhan 430074, China*

(Dated: September 27, 2022)

In this paper we propose a dark-state-based trapping strategy to break the optical diffraction limit for microscopy. We utilize a spatially dependent coupling field and a probe laser field with temporal and spatial modulation to interact with three-level atoms. The temporal modulation allows us to reduce the full width at half maximum (FWHM) of point spread function, and the spatial modulation help us obtain better spatial resolution than Gaussian beam. In addition, we also propose a proof-of-principle experiment protocol and discuss its feasibility.

I. INTRODUCTION

It's well-known that the resolution limit of traditional far-field optical microscopy is about half of the optical wavelength [1], and usually we call it as Rayleigh limit of resolution. The development of related technologies is restricted by such a resolution limit, for example lithography [2], imaging [1] and so on. Several avenues for achieving sub-wavelength spatial resolution are being explored, such as two-photon confocal fluorescence microscopy [3], stimulated emission depletion microscopy [4–6], near-field scanning microscopy [7]. Recently, it has been shown that coherent population trapping or atomic dark state can also be used to achieve super-resolution imaging [8–10]. Position-dependent dark state has been used to obtain the shadow image of a nanometer-scale object embedded in an ultracold atomic medium [10, 11]. The combination of amplitude-modulated probe laser with position-dependent dark state can further increase the spatial resolution [12] of imaging. However, the requirement of full amplitude modulation of probe laser is challenging to achieve in realistic experiments [13]. In this paper, we consider a more general type of temporal and spatial modulation to increase the spatial resolution of atomic imaging. In addition, we also propose a feasible proof-of-principle experiment protocol.

II. BASIC PRINCIPLES

We consider a three-level Λ system interacting with two laser beams that realize a configuration for dark state, as shown in Figure 1. We denote the two ground states of atoms by $|1\rangle$ and $|2\rangle$ while the excited state by $|3\rangle$. The other state $|4\rangle$ is a fluorescence output energy level [10], which allows us to measure the system's state by determining the population of the state $|2\rangle$. One laser beam is a weak probe laser which is on resonance with the transition between $|1\rangle$ and $|3\rangle$ and another one is a strong coupling laser which interacts with $|2\rangle$ and $|3\rangle$. The Rabi frequencies of two laser beams are denoted as $\Omega_p = \Omega_p(x,t)$ and $\Omega_c = \Omega_c(x,t)$ respectively. For simplicity, we consider one-dimensional case, nevertheless it is straightforward to extend the scheme to two-dimensional case.

By means of rotating wave approximation(RAW) [14], the

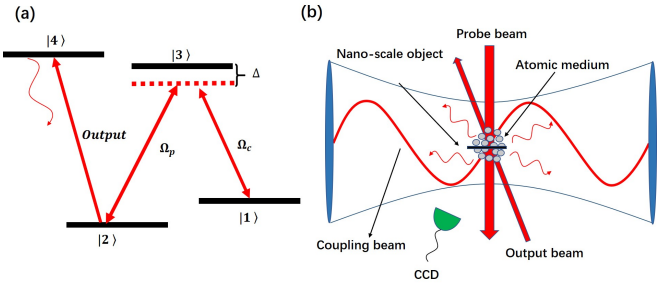

FIG. 1. (a) Energy level diagram. Two laser beams Ω_p and Ω_c are used to interact with atoms and create atomic dark state. Fluorescence laser scatters photons only when atoms are in the state $|2\rangle$, which allows us to detect the population of the state $|2\rangle$. (b) An experiment sketch of atomic miscroscopy. A nanoscale object is embedded in atomic medium. By moving the optical cavity and probe laser simultaneously, we can get a fluorescence shadow image of the object.

Hamiltonian of this system is given as

$$H = \hbar \begin{pmatrix} 0 & 0 & -\frac{\Omega c}{2} \\ 0 & 0 & -\frac{\Omega p}{2} \\ -\frac{\Omega c}{2} & -\frac{\Omega p}{2} & \Delta \end{pmatrix} \tag{1}$$

with Δ is the frequency detunings of both driving fields, see Fig.1(a). If the Rabi frequencies $\Omega_c(x)$ and $\Omega_p(x)$ are time-independent, it is well known that a dark state exist [14]

$$|D\rangle = \frac{\Omega_c(x)}{\sqrt{|\Omega_p(x)|^2 + |\Omega_c(x)|^2}}|1\rangle - \frac{\Omega_p(x)}{\sqrt{|\Omega_p(x)|^2 + |\Omega_c(x)|^2}}|2\rangle. \tag{2}$$

This dark state does not involve any dynamical processes [14]. If we take into account the relaxation processes, no matter what the initial state is, the system will eventually evolve into the dark state as long as the two laser beams are maintained.

It can be seen from (2) that the population of state $|2\rangle$ for the dark state is $P = |\Omega_p(x)|^2 / (|\Omega_p(x)|^2 + |\Omega_c(x)|^2)$. It has been shown that [15] if the coupling beam is a standing-wave $\Omega_c(x) = \Omega_{c0}\sin(kx)$ and the probe beam is a plane wave, the atomic dark state will become position dependent [16]. At the nodes of the standing wave, the population P approaches 1, and the FWHM of this curve is $\Delta x \approx \lambda\,(\Omega_{p0}/\Omega_{c0}) = \lambda/\sqrt{R_0}$

[10] where λ is the wavelength of the coupling beam and the ratio parameter is $\sqrt{R_0} = \Omega_{c0}/\Omega_{p0}$. If R_0 is very large, the FWHM will be far smaller than the wavelength of light and we can use this feature to achieve super-resolution imaging. The spatial resolution can be improved by increasing R_0 and its upper bound was discussed in detail in [17].

Here we assume the probe field is temporally modulated, which can be implemented through Electro-Optics Modulator(EOM) or Acousto-Optic Modulator(AOM) by varying the intensity of the probe laser [13]

$$\Omega_p^2(x,t) = \Omega_{p0}^2(x)\frac{1+\sin(\varphi\cos(\nu t))}{2} \tag{3}$$

where φ and ν is the modulation phase and frequency respectively. In order to discuss the contribution of the main frequency component of $\sin(\varphi\cos(\nu t))$, we expand it with Fourier series,

$$\sin(\varphi\cos(\nu t)) \approx 2J_1(\varphi)\cos(\nu t) - 2J_3(\varphi)\cos(3\nu t) \tag{4}$$

where $J_n(\varphi)$ stands for the n-th order Bessel function of the first kind. We can neglect the second term of (4) if $J_3(\varphi)/J_1(\varphi) \ll 1$ (e. g. φ is in the reasonable range $[0,1]$). We define $A = 2J_1(\varphi)$, thus $0 \le A \le 0.88$.

When the modulation frequency ν is much smaller than the characteristic frequencies [12] of this system, the population P can be calculated by virtue of adiabatic approximation [18]

$$P(x,t) = \frac{1}{1+|\frac{\Omega_c(x)}{\Omega_p(x,t)}|^2} = \frac{\frac{1+A\cos(\nu t)}{2}}{\frac{1+A\cos(\nu t)}{2}+R} \tag{5}$$

where we define $R = |\frac{\Omega_c(x)}{\Omega_{p0}(x)}|^2$. The cosine Fourier coefficients of $P = \sum_{l=0}^{l=\infty} p_l\cos(l\nu t)$ are

$$p_0 = 2 - \frac{4R}{\sqrt{(2R+1)^2 - A^2}}, \tag{6}$$

$$p_1 = \frac{4R\left(-\sqrt{(2R+1)^2-A^2}+2R+1\right)}{A\sqrt{(2R+1)^2-A^2}}, \tag{7}$$

$$p_2 = \frac{4R\left(4R\left(\sqrt{(2R+1)^2-A^2}-2R-1\right)+A^2\right)}{A^2\sqrt{(2R+1)^2-A^2}}. \tag{8}$$

The coefficient $p_l(l = 0,1,2)$ are the function of position x. In our scheme, they can be identified as the point spread functions of this optical system [19]. And the FWHM of the point spread function is a good metric of the spatial resolution of imaging. So if we want to increase the spatial resolution, we should reduce the FWHM of the point spread functions.

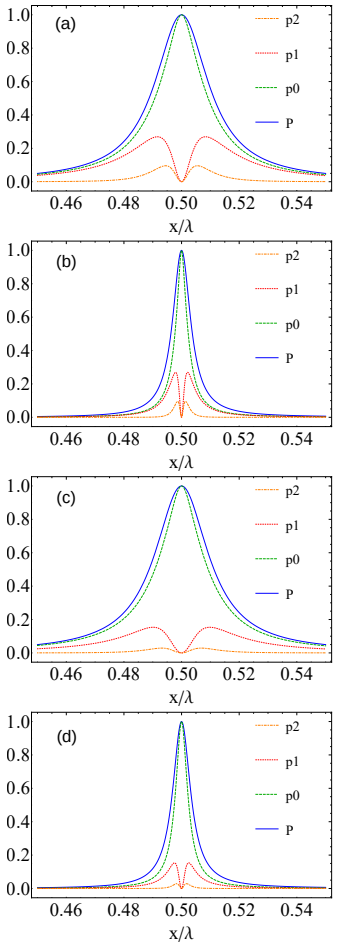

FIG. 2. Normalized point spread functions p_l. Legend: blue solid curve, unmodulated population P ($A = 0$); green dashed curve, DC term (p_0); red dashed curve, coefficient of $\cos\nu t$ (p_1); orange dashed curve, coefficient of $\cos 2\nu t$ (p_2). (a) Gaussian beam, A=0.88; (b) LG beam, A=0.88; (c) Gaussian beam, A=0.573; (d) LG beam, A=0.573.

III. GAUSSIAN AND LAGUERRE-GAUSSIAN LASER

Although we have discuss the case where probe laser is a plane wave, actually it is very difficult to create a perfect plane wave. Instead, usually we use Gaussian beam to serve as the probe laser [10]. The Rabi frequency can be then expressed as $\Omega_{p0}(x) = \Omega\exp(-(\frac{x}{W})^2)$, where W is the beam waist of the probe laser and Ω is a constant. We choose the coupling field to be a standing wave $\Omega_c(x) = \Omega_{c0}\sin(kx)$, and we can obtain $R = R_m(\sin^2(kx)/\exp(-2(\frac{x}{W})^2)$ where $R_m = |\Omega_{c0}/\Omega|^2$. The corresponding point spread functions are plotted in Fig. 2 when $R_m = 100, W = 2\lambda$ which are reasonable values for realistic experiments. It can be seen that higher-order Fourier components offer better resolution, albeit with decreasing intensity of signal. The FWHM becomes larger with the decreasing of modulation coefficient A. Considering the intensity and the FWHM of $p_0(x)$, $p_1(x)$ and $p_2(x)$, it is preferable to use $p_1(x)$ to extract the information

about spatial resolution. When $A = 0.88$, the improvement of the spatial resolution of $p_1(x)$ over the diffraction limit of $\lambda/2$ can reach a factor of 200.

The standing wave profile can be viewed as a kind of spatial modulation for the coupling beam. We further extend our strategy by considering a spatially modulated probe laser. In particular, we consider the first-order Laguerre-Gaussian (LG) beam [20] to serve as the probe field. The Rabi frequency of the probe laser is

$$\Omega_{p0}(x) = \Omega \exp(-(\frac{x}{W})^2)(\frac{x}{W}). \tag{9}$$

The point spread functions are plotted in Fig. 2 when $R_m = 100, W = 2\lambda$. We also use $p_1(x)$ to get the information about spatial resolution. For the chosen value of $A = 0.88$, the spatial resolution can be improved by a factor of about 800 in comparison with the diffraction limit, which represents an enhancement of a factor of 4 as compared with the Gaussian probe laser.

IV. NUMERICAL SIMULATION

In realistic experiments, the impact of relaxation process can not be neglected and the validity of adiabatic approximation also needs to be verified. We adopt a master equation to describe the influence of these factors and simulate the dynamic evolution of a realistic atomic system. Rb-87 atoms trapped in magneto-optical trap (MOT) [21] are utilized to serve as the atomic medium and we choose $|1\rangle \equiv |F = 2\rangle$ and $|2\rangle \equiv |F = 1\rangle$ of the ground electronic state $^5S_{1/2}$. We take the excited state to be $|3\rangle \equiv |F^{'} = 2\rangle$ of the electronic state $^5P_{3/2}$, and the fluorescence output state to be $|4\rangle \equiv |F^{'} = 3\rangle$ of the electronic state $^5P_{3/2}$. The master equation is given as

$$\frac{d}{dt}\rho = -\frac{i}{\hbar}[H, \rho] - \frac{1}{2}(R\rho + \rho R) + \Lambda, \tag{10}$$

where R and Λ are relaxation and repopulation matrix [22].

$$R = \begin{pmatrix} \gamma & 0 & 0 \\ 0 & \gamma & 0 \\ 0 & 0 & \gamma + \Gamma \end{pmatrix}, \tag{11}$$

$$\Lambda = \begin{pmatrix} \gamma/2 + \Gamma\rho_{33}/2 & 0 & 0 \\ 0 & \gamma/2 + \Gamma\rho_{33}/2 & 0 \\ 0 & 0 & 0 \end{pmatrix}, \tag{12}$$

where γ is the atomic diffusion rate and Γ is the decay rate of the excited state. For Rb-87, $\Gamma = 2\pi \times 5.7$ MHz and it is reasonable for us to choose $R_0 = 100, W = 2\lambda, \Omega = 100$ MHz, $\Delta = 5$ MHz, $A = 0.88$, $\gamma = 2\pi \times 10$ Hz [15]. Assuming that at $t = 0$, all atoms are in the state $|2\rangle$. Because the density matrix ρ is dependent on the position x, we choose $x = 0.497\lambda$. For $\nu = 2\pi \times 1$ MHz, $\nu = 2\pi \times 100$ kHz and $\nu = 2\pi \times 10$ kHz, we can solve (10) to calculate the population $P = \langle 2|\rho|2\rangle$, in comparison with the results obtained from the adiabatic approximation shown in Fig. 3. It can be seen that when $\nu = 2\pi \times 1$ MHz, the adiabatic approximation is not valid. However, if ν reduces to $2\pi \times 100$ kHz, the simulation result from the master equation agrees well with the adiabatic approximation. Therefore, the scheme can achieve good performance when the modulation frequency ν is below $2\pi \times 100$ kHz.

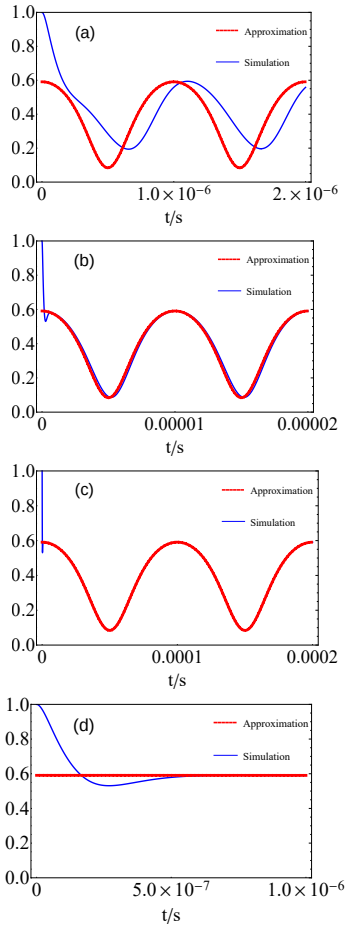

FIG. 3. The population of the state $|2\rangle$ from the simulation of the master equation (blue curves) as compared with the adiabatic approximation (red curves) for the modulation frequency (a) $\nu = 2\pi \times 1$ MHz; (b) $\nu = 2\pi \times 100$ kHz; (c) $\nu = 2\pi \times 10$ kHz; (d) is a zoom in of the temporal profile of (c), which shows that the system takes about 800 ns to evolve into dark state.

V. EXPERIMENT SEQUENCE

Based on the above analysis, we choose $\nu = 2\pi \times 10$ kHz and present a simple experimental protocol: (1) Use magneto-optical trap (MOT) to trap and cool down the system. (2) Use EOM or AOM to induce modulation. (3) Apply both probe and coupling beams to prepare the system into the dark state, and the duration of two laser beams is about 1000 ns because the system spends about 800ns to evolve into dark state, see Fig.3 (d). (4) Apply the readout laster pulse ($\sim$500 ns) to get information on the population P of the state $|2\rangle$. (5) Repeat

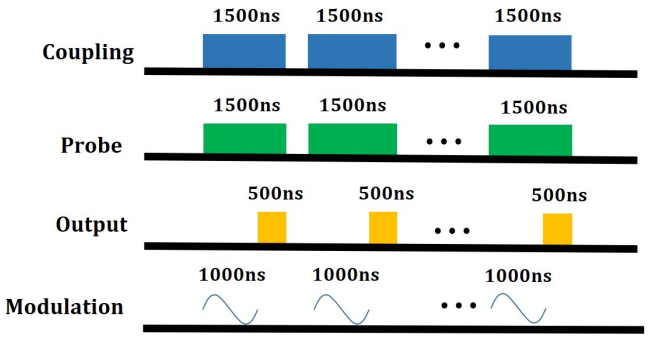

FIG. 4. Experiment sequence. The AOM or EOM signal is shown as sinusoidal function, and the other laser beams are shown as pulses.

these procedures until we sample one period of the population P. (6) Move the probe laser and the optical cavity simultaneously to scan the nanoscale object. The experiment sequence is shown in Fig. 4.

VI. SUMMARY

In conclusion, we propose to achieve sub-wavelength resolution atomic imaging by modulating the temporal and spatial profiles of the probe laser. By means of temporal and spatial modulation, we show that the FWHM of the point spread function can be significantly reduced. As compared with the previous schemes [10–12], our strategy is more feasible to achieve a better spatial resolution. In addition, we would like to point out that our method can also be used to improve the spatial resolution of atomic probability density microscopy.

[1] M. Born and E. Wolf, *Principles of optics: electromagnetic theory of propagation, interference and diffraction of light* (Elsevier, 2013).
[2] C. Mack, *Fundamental principles of optical lithography: the science of microfabrication* (John Wiley & Sons, 2008).
[3] W. Denk, J. H. Strickler, and W. W. Webb, Two-photon laser scanning fluorescence microscopy, Science **248**, 73 (1990).
[4] T. A. Klar, S. Jakobs, M. Dyba, A. Egner, and S. W. Hell, Fluorescence microscopy with diffraction resolution barrier broken by stimulated emission, Proceedings of the National Academy of Sciences **97**, 8206 (2000).
[5] S. W. Hell and M. Kroug, Ground-state-depletion fluorscence microscopy: A concept for breaking the diffraction resolution limit, Applied Physics B **60**, 495 (1995).
[6] S. W. Hell and J. Wichmann, Breaking the diffraction resolution limit by stimulated emission: stimulated-emission-depletion fluorescence microscopy, Optics letters **19**, 780 (1994).
[7] U. Dürig, D. W. Pohl, and F. Rohner, Near-field optical-scanning microscopy, Journal of applied physics **59**, 3318 (1986).
[8] C. Liu, S. Gong, D. Cheng, X. Fan, and Z. Xu, Atom localization via interference of dark resonances, Physical Review A **73**, 025801 (2006).
[9] H. Li, V. A. Sautenkov, M. M. Kash, A. V. Sokolov, G. R. Welch, Y. V. Rostovtsev, M. S. Zubairy, and M. O. Scully, Optical imaging beyond the diffraction limit via dark states, Physical Review A **78**, 013803 (2008).
[10] D. Yavuz and N. Proite, Nanoscale resolution fluorescence microscopy using electromagnetically induced transparency, Physical Review A **76**, 041802 (2007).
[11] K. Stokes, C. Schnurr, J. Gardner, M. Marable, G. Welch, and J. Thomas, Precision position measurement of moving atoms using optical fields, Physical review letters **67**, 1997 (1991).
[12] K. T. Kapale and G. S. Agarwal, Subnanoscale resolution for microscopy via coherent population trapping, Optics letters **35**, 2792 (2010).
[13] B. E. Saleh and M. C. Teich, *Fundamentals of photonics* (John Wiley & Sons, 2019).
[14] M. O. Scully and M. S. Zubairy, Quantum optics (1999).
[15] A. V. Gorshkov, L. Jiang, M. Greiner, P. Zoller, and M. D. Lukin, Coherent quantum optical control with subwavelength resolution, Physical review letters **100**, 093005 (2008).
[16] Y. Wang, S. Subhankar, P. Bienias, M. Łącki, T.-C. Tsui, M. A. Baranov, A. V. Gorshkov, P. Zoller, J. V. Porto, S. L. Rolston, *et al.*, Dark state optical lattice with a subwavelength spatial structure, Physical review letters **120**, 083601 (2018).
[17] G. S. Agarwal and K. T. Kapale, Subwavelength atom localization via coherent population trapping, Journal of Physics B: Atomic, Molecular and Optical Physics **39**, 3437 (2006).
[18] J. J. Sakurai and E. D. Commins, Modern quantum mechanics, revised edition (1995).
[19] J. W. Goodman, *Introduction to Fourier optics* (Roberts and Company Publishers, 2005).
[20] L. Allen, M. W. Beijersbergen, R. Spreeuw, and J. Woerdman, Orbital angular momentum of light and the transformation of laguerre-gaussian laser modes, Physical Review A **45**, 8185 (1992).
[21] J. Miles, Z. Simmons, and D. Yavuz, Subwavelength localization of atomic excitation using electromagnetically induced transparency, Physical Review X **3**, 031014 (2013).
[22] M. Auzinsh, D. Budker, and S. Rochester, *Optically polarized atoms: understanding light-atom interactions* (Oxford University Press, 2010).